Available online at www.sciencedirect.com
ScienceDirect
Journal of Sound and Vibration 321 (2009) 405–415
JOURNAL OF SOUND AND VIBRATION
www.elsevier.com/locate/jsvi

Lower-bound on SNR of the *n*th-order hyperbolic time–frequency kernel

Khoa N. Le*

Centre for Wireless Monitoring and Applications, Griffith School of Engineering, Griffith University, Gold Coast Campus, Parklands Drive, Southport, QLD 4222, Australia

Received 31 January 2008; received in revised form 21 August 2008; accepted 15 September 2008
Handling Editor: J. Lam
Available online 25 October 2008

Abstract

An estimate of the lower-bound on signal-to-noise ratio (SNR) of the *n*th-order hyperbolic time–frequency kernel is given. The effects of kernel parameters such as β, τ, n and a on the SNR are discussed. In particular, the direct relationship between the SNR and auto-term slope a is studied in detail. Conditions under which the lower-bound on SNR is obtained are derived. Preliminary observations on a transfer function model with the auto-term slope a and β as inputs, and lower-bound on SNR as output are given. Possible further work is outlined.

1. Introduction

Some properties of the hyperbolic time–frequency kernel was reported recently [1] to show its effectiveness in suppressing cross terms, supporting auto-terms and its superior noise robustness compared to the popular Choi–Williams kernel [2] in the time–frequency plane. In Ref. [1], the SNR (signal-to-noise ratio) of the first-order hyperbolic, Choi–Williams and *n*th-order hyperbolic kernels including the conditions for optimal SNR were reported which form the foundation for the work on the hyperbolic kernel family reported here. Current works on time–frequency kernels' SNR are scarcely found in the literature, except the early works by Amin [3] published in 1996 and Stankovic [4] in 1997, leading to works reported in Refs. [1,5]. The main difficulty with research work on time–frequency kernels' SNR is its mathematical complexity. However, kernel noise robustness truly reflects their behaviour and characteristics under noisy conditions which are commonly encountered in practice and should be considered as an important aspect in choosing kernels for various signal-processing applications. Another indirect reason is that not many time–frequency kernels have been proposed in the last decade with the last kernel, prior to the proposal of the hyperbolic kernel in 2003 [5], was proposed by Costa [6] in 1995. Further, it is also widely believed that SNR is the key factor in determining the effectiveness and performance of signal-processing tools.

*Tel.: +61 7 5552 9175; fax: +61 7 5552 8065.
E-mail address: K.Le@griffith.edu.au

0022-460X/$ - see front matter
doi:10.1016/j.jsv.2008.09.038

The motivation for this work is of three-fold. First, even though the hyperbolic kernel was proposed in Ref. [5] and studied in detail in Ref. [1], its numerical lower-bound on SNR was not available. Although the upper-bound SNR [1] of the nth-order hyperbolic kernel has been successfully estimated, it is necessary to estimate the lower-bound on SNR so that the robustness range of the kernel is clearly identified. Second, the effectiveness of the first-order hyperbolic [1,5,7] kernel compared to the Choi–Williams kernel motivates more work on higher-order hyperbolic family members so that their effectiveness and features are thoroughly explored. Third, as reported in Refs. [5,7], there exists a relationship between time–frequency kernels and wavelets which enables the generation of new wavelets from new kernels and vice versa. From the second point above, by estimating kernels' noise-robust range, i.e. lower-bound and upper-bound on SNR, it is possible to establish a benchmark for various different time–frequency kernels and wavelets. By using such a benchmark, a systematic comparison in terms of cross-term suppression, auto-term support and noise robustness of various kernels can be made. From the wavelet point of view, it is also possible to classify various different types of wavelet families based on their noise robustness. It is worthy to note that: (i) the lower bound on SNR is more important than the upper bound as the lower bound represents the weakness of the kernel and indicates the critical threshold which should not be crossed when employing the kernel for signal processing applications, and (ii) from this paper perspective, the lower bound on SNR represents the maximum noise level which can be tolerated by the kernel. Additional increase in the noise level would severely degrade the kernel's performance. By saying that, the lower bound on SNR is more useful than the upper bound. In this paper, only real noise sources are considered.

The paper is organised as follows. Section 2 briefly gives the background on Cohen's time–frequency power spectra. Section 3 defines the general expression of an auto-term function and gives the mathematical expression of the auto-term function of the nth-order hyperbolic kernel. Section 4 gives the background on the hyperbolic kernel family and the conditions under which noise immunity is achieved. Section 5 presents the main findings of the paper in which detailed analyses of the lower-bound on SNR are given. In addition, detailed conditions governing the lower-bound on SNR are discussed. Section 6 summarises the findings of the paper and outlines possible extensions.

2. Background on Cohen's time–frequency distribution

Cohen's time–frequency distributions are used to study non-stationary signals whose statistical properties such as mean and variance vary with time. By using time–frequency distributions or time–frequency power spectra, it is possible to study properties of multi-component signals as time and frequency vary. The general form of Cohen's time–frequency distribution is defined as [8,9]

$$P(t,\omega)=\frac{1}{4\pi^2}\int_{-\infty}^{+\infty}\int_{-\infty}^{+\infty}\int_{-\infty}^{+\infty}\mathrm{e}^{-j\theta t-j\tau\omega+j\theta u}\Phi(\theta,\tau)R_{t,1}(t,\tau)\,\mathrm{d}u\,\mathrm{d}\tau\,\mathrm{d}\theta, \tag{1}$$

where $\Phi(\theta,\tau)$ is the kernel function which can be used to significantly shape the time–frequency distribution, $R_{t,1}(t,\tau)=x(u+(\tau/2))x^*(u+(\tau/2))$ which is the auto-correlation function of the input analytic signal $x(t)$, $u=t+(\tau/2)$, τ the lag parameter, and t the running time variable. It is also clear from Eq. (1) that the characteristics of $P(t,\omega)$ are uniquely and significantly dependent on $\Phi(\theta,\tau)$. Eq. (1) can also be rewritten as

$$P(t,\omega)=\frac{1}{4\pi^2}\int_{-\infty}^{+\infty}\int_{-\infty}^{+\infty}\int_{-\infty}^{+\infty}\underbrace{[\mathrm{e}^{-j\theta(t-u)}\Phi(\theta,\tau)]}_{W(t-u,\tau)}\mathrm{e}^{-j\tau\omega}R_{t,1}(t,\tau)\,\mathrm{d}u\,\mathrm{d}\tau\,\mathrm{d}\theta. \tag{2}$$

From Eq. (2), it is clear that the parameter $(t–u)$ is used as a temporary frequency parameter in the Fourier transform operation with respect to θ to obtain the weighting function of $\Phi(\theta,\tau)$ as a function of $(t–u)$ and τ. It is also clear that ω is the operator used to generate the Fourier transform of $\Phi(\theta,\tau)$ with respect to τ. In this paper, to estimate the lower-bound SNR of the nth-order hyperbolic kernel, the condition $\omega=(t–u)$ is used as carried out in Section 4.

3. Auto-term function of the *n*th-order hyperbolic kernel

The *n*th-order hyperbolic kernel is given as

$$\Phi_{Hy\_g}(\theta,\tau)=[\mathrm{sech}(\beta\theta\tau)]^n, \tag{3}$$

where n is the order of the kernel, β the control parameter, θ and τ variables. It should be noted that the hyperbolic kernel family has been shown as valid kernels for Cohen's time–frequency distributions [5,7,10].

The auto-term function of a kernel is defined as [1,3,4]

$$\text{Auto-term function}=\int_{-\infty}^{+\infty}\Phi(\theta,\tau)\Big|_{\theta=-a\tau}\mathrm{e}^{-j\omega\tau}\,\mathrm{d}\tau, \tag{4}$$

where a is the auto-term slope. Because Eq. (1) is applicable for multi-component signals, so is Eq. (4). In other words, Eq. (4): (i) can be considered as independent of the input signal and only dependent on the time–frequency kernel, and (ii) truly reflects the kernel ability on supporting auto-terms. By substituting $\theta=-a\tau$, the kernel becomes a one-dimensional function of τ, i.e. the kernel energy can now be estimated either in the time or frequency plane. Imagine a straight line going through the origin with a slope a. As a is varied, so is the area under the curve. Thus, the auto-terms represent the signal energy as this straight line sweeps through the first quarter of the plane, assuming $a>0$. In other words, the auto-terms can be considered as instantaneous signal energy which is proportional to the instantaneous frequency. By replacing $\Phi(\theta,\tau)$ with $\Phi_{Hy\_g}(\theta,\tau)$ and letting $\theta=-a\tau$, the auto-term function of the *n*th-order hyperbolic kernel is obtained. The auto-term function is used to study the location, distribution and magnitude of auto-terms of multiple non-stationary signals in the time–frequency plane. For symmetrical kernels such as the hyperbolic and Choi–Williams, the auto-term function can be approximately used as signal power to estimate the SNR [1] because the area under the curve of the weighting functions of these kernels approximately approaches unity. As a result, the SNR's of the hyperbolic and Choi–Williams kernels are directly proportional to their auto-term functions as clearly shown in Ref. [1]. The auto-term and weighting functions of the *n*th-order hyperbolic kernel are given by (Ref. [1]) as

$$\mathrm{AUTO}_{Hy\_g}=\int_{-\infty}^{\infty}[\mathrm{sech}(\beta a\tau^2)]^n\mathrm{e}^{-j\omega\tau}\,\mathrm{d}\tau, \tag{5}$$

$$W_{Hy\_g}(\tau,t-u)=\beta\pi\left\{\mathrm{sech}\left(\frac{\pi(t-u)}{2\beta\tau}\right)\prod_{m=1}^{n}\left[\left(m-\frac{1}{2}\right)^2+\left(\frac{t-u}{2\beta\tau}\right)^2\right]\right\}\times\left\{\frac{-n^2\times 2^{2n}}{(2n)!}+\frac{2^{2n+1}\times n(n+1)}{(2n+4)!}\left[5+8n+4n^2+\left(\frac{t-u}{\beta\tau}\right)^2\right]\right\}, \tag{6}$$

where $n=1, 3, 5, 7,\ldots$.

Subsequent changes in variables as can be seen in Eq. (1) make Cohen's time–frequency power spectrum to be a function of t and ω which can be conveniently used for signal analyses. In this paper, the intermediate form of the weighting function is used to form the relationship among (t–u), ω and τ. From that, it is possible to work out the lower-bound on SNR of $\Phi_{Hy\_g}(\theta,\tau)$.

4. Maximum theoretical SNR

It was shown in Ref. [1] that the area under the curve of the hyperbolic and Choi–Williams kernels is unity which significantly simplifies their SNR expressions. However, to estimate the lower-bound SNR of the *n*th-order hyperbolic kernel, the general expression of the weighting function should be used. For real noise sources, the variance σ^2 of the time–frequency distribution is given as a function of the noise variance ${\sigma_x}^2$ as [4]

$$\sigma^2(\omega)=\sigma_x^4\sum_{\tau=-\infty}^{+\infty}\sum_{x=-\infty}^{+\infty}|W(\tau,x)|^2, \tag{7}$$

where $x = t–u$, yielding

$$\frac{\sigma^2(\omega)}{\sigma_x^4} = \sum_{\tau=-\infty}^{+\infty}\sum_{x=-\infty}^{+\infty} |W(\tau,x)|^2. \tag{8}$$

Eq. (8) gives the distribution-to-noise ratio (DNR) which does not include the effects of auto-terms. To consider these effects, the auto-term values are required. Using Eqs. (5) and (8), the SNR of the nth-order hyperbolic kernel can be mathematically given as

$$\mathrm{SNR}_{Hy\_g} = \frac{\mathrm{AUTO}_{Hy\_g}}{\int_{-\infty}^{+\infty}\int_{-\infty}^{+\infty}[W_{Hy\_g}(\tau,x)]^2\,\mathrm{d}x\,\mathrm{d}\tau}, \tag{9}$$

which can be maximised by forcing the weighting function (Eq. (6)) to be zero or by maximising the auto-term function (Eq. (5)).

For analytic external noise sources, after some algebraic manipulations, the SNR of the nth-order hyperbolic kernel is mathematically given as [4]

$$\mathrm{SNR}_{Hy\_g}^{\mathrm{Analytic}} = \frac{1}{2\pi^2}\frac{\mathrm{AUTO}_{Hy\_g}}{\int_{-\pi}^{+\pi}\int_{-|2\omega-\tau|}^{|2\omega-\tau|}[W_{Hy\_g}(\tau,x)]^2\,\mathrm{d}x\,\mathrm{d}\tau}. \tag{10}$$

It should be noted that the SNR for the case of analytic noise as given in Eq. (10) is of the same mathematical form as of Eq. (9) but with different: (i) integration limits because $|\omega| < \pi/2$, and (ii) modification constant. At the first glance, Eq. (10) appears to be $2\pi^2$ times smaller than Eq. (9) but because its integration limits are narrower than those of Eq. (9), thus the value of Eq. (10) is not necessary smaller than that of Eq. (9). In fact, they both can be identically employed as performance indicators as was shown in Ref. [4]. In this paper, only real external noise sources are considered. Another point to note is that Eqs. (9) and (10) can be easily extended for multi-component signals by taking the average SNR as given in Eqs. (11) and (12), respectively, as

$$\mathrm{SNR}_{Hy\_g} = \frac{1}{N}\sum_{i=1}^{N}\mathrm{SNR}_{Hy\_g(i)} \tag{11}$$

and

$$\mathrm{SNR}_{Hy\_g}^{\mathrm{Analytic}} = \frac{1}{N}\sum_{i=1}^{N}\mathrm{SNR}_{Hy\_g(i)}^{\mathrm{Analytic}}, \tag{12}$$

where N is the number of individual signals in the composite multi-component signal.

From Eq. (7), it is also clear that another way to derive the SNR is to determine the formula of the noise variance in terms of the distribution variance and weighting function, which is given as

$$\sigma_x^4 = \frac{\sigma^2(\omega)}{\sum_{\tau=-\infty}^{+\infty}\sum_{x=-\infty}^{+\infty}|W(\tau,x)|^2}. \tag{13}$$

The SNR is then given as

$$\mathrm{SNR} = \frac{\mathrm{AUTO}}{\sigma_x^4} = \left(\frac{\mathrm{AUTO}}{\sigma^2(\omega)}\right)\sum_{\tau=-\infty}^{+\infty}\sum_{x=-\infty}^{+\infty}|W(\tau,x)|^2, \tag{14}$$

which is also a useful formula for the SNR. Eqs. (11) and (12) can be employed to further extend Eq. (14) for multi-component signals. However, because of: (i) its independence of the input signals, (ii) its only dependence on the time–frequency kernel, and (iii) easy of computation, only Eq. (9) is considered in this paper.

From Eq. (6), to obtain the optimal SNR for the kernel, the relationship between $(t–u)$ and τ as a function of β and n is given by [1]

$$t - u = \beta\tau\sqrt{8n^4 + 32n^3 + 34n^2 + 4n - 5}, \quad \text{where } n = 1, 3, 5, 7, \ldots, \tag{15}$$

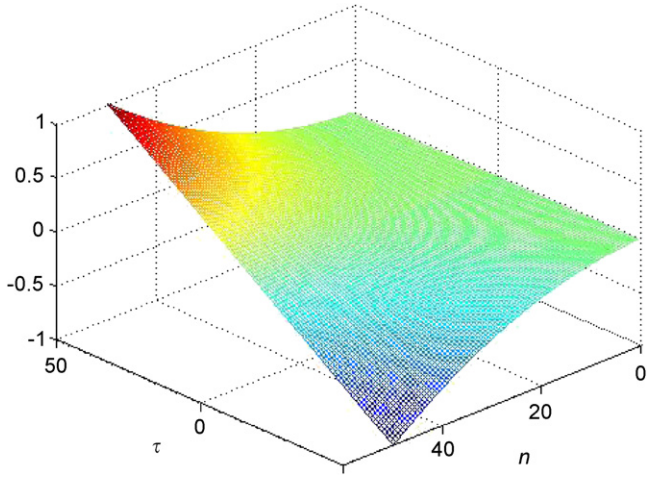

Fig. 1. Graphical representation of normalized $(t–u)$ (Eq. (15)) against τ and $0<n<50$ with $\beta=1$, yielding a theoretical SNR of infinity.

which is plotted in Fig. 1. It should also be noted that under the condition imposed by Eq. (15), the SNR attains its maximum theoretical value of infinity, i.e. yielding complete noise immunity to the kernel, and is independent of the auto-term slope a. It is also clear that from Eq. (6), the lower-bound and upper-bound on SNR's are strongly dependent on the area under the squared weighting function because the area under the auto-term function is usually much smaller as will be seen later. Mathematically, Eq. (5) can be rewritten in terms of sin and cos functions as

$$\mathrm{AUTO}_{Hy\_g}=2\int_0^{+\infty}\{[\mathrm{sech}(\beta a\tau^2)]^n\cos(\omega\tau)-j[\mathrm{sech}(\beta a\tau^2)]^n\sin(\omega\tau)\}\,\mathrm{d}\tau, \tag{16}$$

in which the second term does not contribute to the integral in Eq. (16) because sech and sin are even and odd functions, respectively, yielding their product an odd function. Thus, Eq. (16) can then be rewritten as

$$\mathrm{AUTO}_{Hy\_g}=2\int_0^{+\infty}[\mathrm{sech}(\beta a\tau^2)]^n\cos(\omega\tau)\,\mathrm{d}\tau, \tag{17}$$

which means that the Fourier transform of $[\mathrm{sech}(a\beta\tau^2)]^n$ is real.

5. Lower-bound on SNR

The lower-bound on SNR of the nth-order hyperbolic kernel can be obtained by using a change of variable from ω to $(t–u)$ as explained earlier. By using Eq. (15) under the optimal SNR condition and replacing ω with $(t–u)$ for modification and simplification purposes, the auto-term function can be rewritten in terms of τ, β, a and n as

$$\mathrm{AUTO}_{Hy\_g}=2\int_0^{+\infty}[\mathrm{sech}(a\beta\tau^2)]^n\cos(\beta\tau^2\sqrt{8n^4+34n^3+32n^2+4n-5})\,\mathrm{d}\tau. \tag{18}$$

By using $k=(t–u)/\tau$, Eq. (6) can be rewritten as

$$W_{Hy\_g}(k)=\beta\pi\left\{\mathrm{sech}\left(\frac{\pi k}{2\beta}\right)\prod_{m=1}^{n}\left[\left(m-\frac{1}{2}\right)^2+\left(\frac{k}{2\beta}\right)^2\right]\right\}\left\{\frac{2^{2n+1}n(n+1)}{(2n+4)!}\left[\left(\frac{k}{\beta}\right)^2+5+8n+4n^2\right]-\frac{n^2 2^{2n}}{(2n)!}\right\}, \tag{19}$$

Hence Eq. (9) can be rewritten as

$$\mathrm{SNR}_{Hy\_g}=\frac{\mathrm{AUTO}_{Hy\_g}}{2\int_0^{+\infty}[W_{Hy\_g}(k)]^2\,\mathrm{d}k}. \tag{20}$$

To determine the lower-bound on SNR, the condition of attaining a local maximum in $[W_{Hy\_g}(k)]^2$ is required, which is the root of

$$\mathrm{d}[W^2_{Hy\_g}(k)]/\mathrm{d}k = 0, \tag{21}$$

yielding the largest root given by

$$k = \frac{t-u}{\tau} = \beta\sqrt{0.37 + 1.2n + n^2}. \tag{22}$$

It should be noted that in obtaining Eq. (22), it is assumed that the roots of Eq. (21) are large [11] which also means that Eq. (22) is linear in terms of n. It is evident that Eq. (22) yields a linear relationship between k and n for the worst condition, under which the kernel's squared weighting function attains its maximum, as compared to the quadratic relationship between k and n given in Eq. (6) in which the weighting function attains its minimum value of zero. Eq. (22) is then substituted into Eq. (19) yielding the maximum squared weighting function. After that, Eq. (20) is used to estimate numerical values of the lower-bound on SNR as a function of a. It should be noted that the magnitude of the auto-term function is independent of the maximum value of the weighting function, but strongly dependent on the auto-term slope a as will be seen later.

By using the condition given in Eq. (22), the auto-term function can be estimated as

$$\mathrm{AUTO}_{Hy\_g} = 2\int_0^{+\infty} [\mathrm{sech}(a\beta\tau^2)]^n \cos(\beta\tau^2\sqrt{n^2 + 1.2n + 0.37})\,\mathrm{d}\tau, \tag{23}$$

and plotted in Fig. 2 for $a = 1$, from which it is evident that the auto-term function attains a larger magnitude, thus yielding a larger lower-bound on SNR than its theoretical value. However, since the theoretical value of the SNR cannot be obtained, a "soft" lower-bound on SNR may be considered to be satisfactory in this case. The lower-bound on SNR can be obtained by taking the ratio of the area under the curve of the auto-term function and the area under the curve of the squared weighting function $[W_{Hy\_g}(k)]^2$. It should be noted that the maximum value of $[W_{Hy\_g}(k)]^2$ is independent of a (Fig. 3).

Simulation results show that the general shape of the kernel's squared weighting function is strongly dependent on β and less dependent on n as its value rapidly decreases to zero as β increases. Therefore, to reduce mathematical complexity, it is sensible to assign a large value to β so that the denominator of Eq. (9) is only dependent on n. Thus, Eq. (9) can be rewritten as

$$\mathrm{SNR}_{Hy\_g} = \frac{\mathrm{AUTO}_{Hy\_g}}{\int_0^{+\infty} 2[W_{Hy\_g}(k,n)]^2\,\mathrm{d}k}. \tag{24}$$

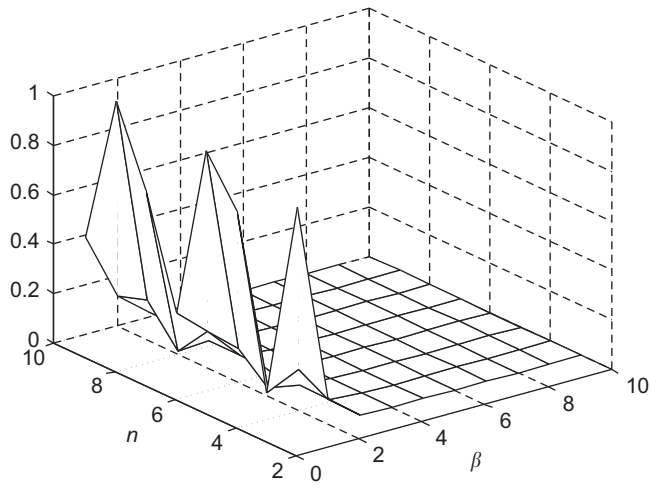

Fig. 2. Normalised auto-term function with $a = 1$ under the optimal condition imposed by Eq. (15). The auto-term function's shape remains largely unchanged for other values of a.

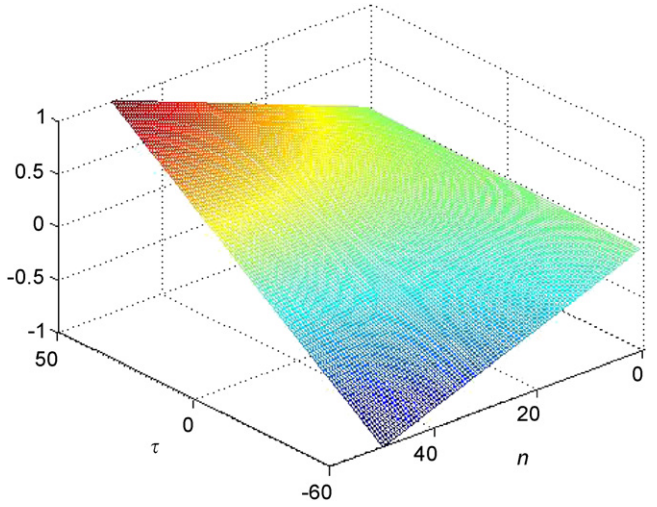

Fig. 3. Plotting of normalized k (Eq. (22)) as a function of τ and n with $\beta = 1$.

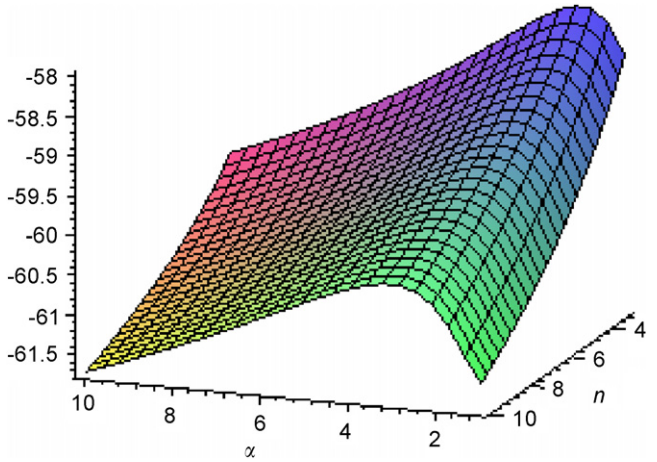

Fig. 4. Lower-bound on SNR in dB as a function of a and n under the conditions imposed by Eq. (22) and with $\beta = 1$. The lower-bound on SNR swings between -58 and -61.5 dB.

By substituting Eq. (22) into Eq. (19), the approximate numerical constant value of 1,769,877 with $\beta = 100$ for the area under the curve of the function $[W_{Hy\_g}(k)]^2$ is obtained, which is independent of the auto-term slope a. The lower-bound on SNR is then estimated by taking the ratio of the numerical value of AUTO_{Hy_g}, given by Eq. (23), and 1,769,877. The lower-bound on SNR as a function of a and n with $\beta = 1$ is plotted in Fig. 4, from which it decreases as n increases. For other values of β, the lower-bound on SNR resembles the shape of the bound in Fig. 4, but has a different magnitude. Fig. 5 plots the lower-bound on SNR as a function of β with $a = 3$, from which a linear relationship between the parameters is observed.

From Fig. 4, by fixing β, the lower-bound on SNR significantly decreases with the order n, with the peak located at $a \approx 3$. It should also be noted that fixing β and plotting the lower-bound on SNR with a and n is not useful since the kernel family becomes severely less noise robust as n increases. From Fig. 5, the relationship between the lower-bound on SNR and β is linear in log–log scales which suggests that their transfer function could be modelled as a sum of exponentials. From simulation results, by fixing a, the lower-bound on SNR remains almost constant as n increases. However, it rapidly decreases with β. Under this condition, the lower-bound on SNR is more stable than fixing β as displayed in Fig. 4. Thus, it is appropriate and advantageous to

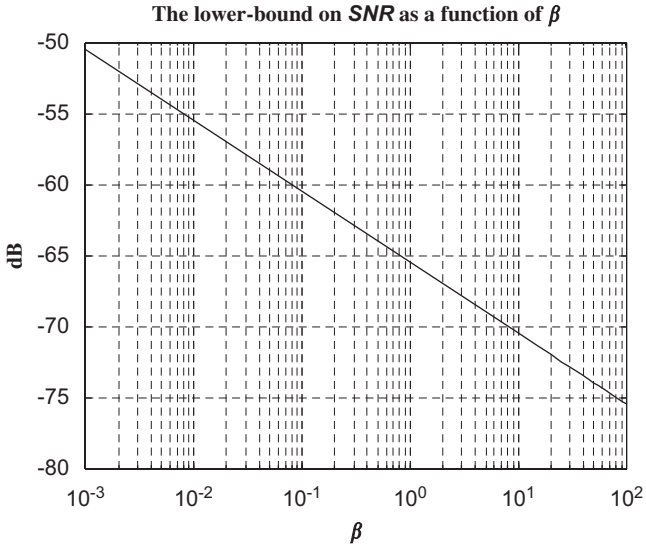

Fig. 5. Linear relationship in log–log scales between the lower-bound on SNR and β under the conditions imposed by Eq. (22) with $a = 3$, corresponding to the peak of the lower-bound on SNR as shown in Fig. 4.

fix a and examining the lower-bound on SNR in terms β and n. It should also be stressed that n should not be fixed as that would limit the degree of freedom in exploring the characteristics of kernel members.

Even though the main focus of this paper is to estimate the lower-bound on SNR of the nth-order hyperbolic kernel, it is worth to preliminarily examine the relationship between a and the lower-bound on SNR, i.e. a relation between a and the SNR at a particular value of n, which helps forming the foundation for future research directions on the kernel family. This can be achieved by fixing a and plotting the lower-bound on SNR as a function of β and n. For other values of the auto-term slope a, the shape (but not its magnitude) of the auto-term function and SNR under the condition imposed by Eq. (22) remain unchanged.

Table 1 summarises the measured lower-bound on SNR of the nth-order hyperbolic kernel as a function of a.

To relate a and the lower-bound on SNR, a transfer function is required which can be obtained by applying a simple polynomial curve fitting method provided in MATLAB to the given data in Table 1.

Fig. 6 plots the lower-bound on SNR as a function of a under the condition imposed by Eq. (22) and an approximate fifth-order polynomial transfer function. The approximate curve fitting can be significantly improved by increasing the order of the polynomial to 20 as shown in Fig. 7. As can be seen in Fig. 6, the lower-bound on SNR decreases as a increases which is consistent with the results reported in Refs. [1,5,7,10].

Mathematically, the transfer functions relating the lower-bound on SNR to a by using the fifth- and 20th-order polynomial curve fitting methods are given by Eqs. (25) and (26) as

$$H_{5th} = 0.0003a^3 - 0.0112a^2 + 0.0439a - 66.5712, \tag{25}$$

and

$$H_{20th} = 0.0004a^7 - 0.0093a^6 + 0.0878a^5 - 0.4581a^4 + 1.2315a^3 - 1.3108a^2 + 0.7745a - 66.7427. \tag{26}$$

Eqs. (25) and (26) give simple mathematical models of the transfer function of a system relating the auto-term slope a as the input to the lower-bound on SNR as the output. It is also clear that the 20th-order polynomial fitting to the given data yields a more accurate fitting than the fifth-order polynomial method. In addition, for orders larger than twenty, the method does not give more accurate fitting results. At this point, one may ask whether the system is linear time invariant (LTIV) so that control- and circuit-theory tools can be directly applied to it. It should be stressed that the main focus of this paper is to estimate the lower-bound on SNR as a function of a and β, and thus, the discussion on modelling of the transfer function relating the two

Table 1
Measured lower-bound on SNR in dB as a function of a

a	SNR (dB)	a	SNR (dB)	a	SNR (dB)
0	–66.6793	12	–67.1646	26	–68.6773
0.1	–66.6759	12.5	–67.1903	28	–68.9576
0.2	–66.6248	13	–67.229	29	–68.9576
0.3	–66.5911	14	–67.4009	30	–69.0159
0.4	–66.5688	15	–67.5379	35	–69.3619
0.5	–66.5688	16	–67.6364	40	–69.6873
0.6	–66.5699	17	–67.8108	45	–69.9219
0.7	–66.5135	18	–67.931	50	–70.099
0.8	–66.4697	19	–68.1337	60	–70.4929
0.9	–66.4588	19.5	–68.0861	70	–70.8958
1	–66.4372	20	–68.1337	80	–71.1122
10	–66.7045	22	–68.414	90	–71.3735
11	–66.9044	24	–68.5878		

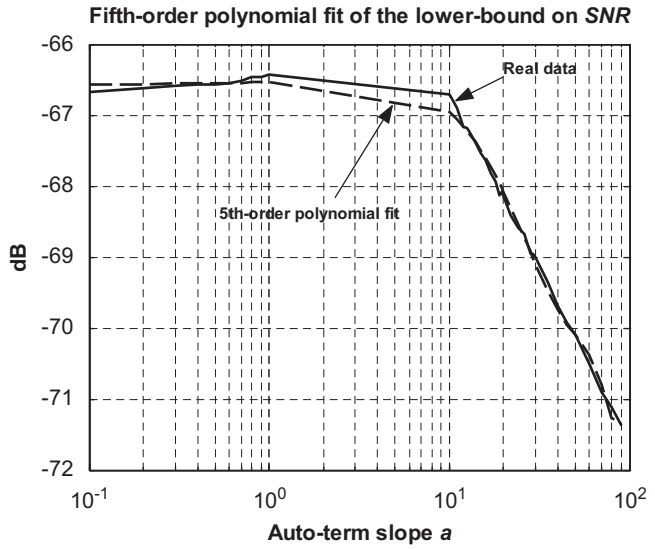

Fig. 6. Fifth-order polynomial fit of the lower-bound on SNR as a function of a on log–log scales under the condition imposed by Eq. (22).

parameters should be temporarily stopped here. More work is currently in progress to thoroughly investigate this relationship and will be reported in a separate publication.

To assess the effectiveness of the hyperbolic and Choi–Williams kernels, other recent kernels are considered. The mathematical forms of some recent kernels are given as follows:

$$\text{Born-Jordan}: \quad \Phi_{\text{BJ}}(\theta,\tau)=\frac{\sin(\theta\tau/2)}{\theta\tau/2}, \tag{27}$$

$$\text{Sinc}: \quad \Phi_{S}(\theta,\tau)=\text{rect}(\theta\tau/\alpha), \tag{28}$$

$$\text{Butterworth}: \quad \Phi_{\text{BW}}(\theta,\tau)=\frac{1}{1+(\theta\tau/\theta_0\tau_0)^4}, \tag{29}$$

where α, $\theta_0\tau_0$ are kernel parameters.

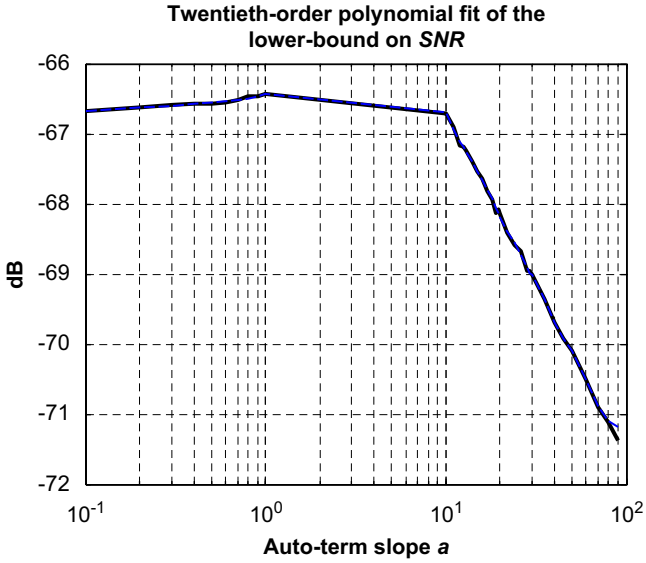

Fig. 7. Twentieth-order polynomial fit of the lower-bound on SNR on log–log scales under the condition imposed by Eq. (22). The fitting is much more accurate than the fifth-order fitting plotted in Fig. 6.

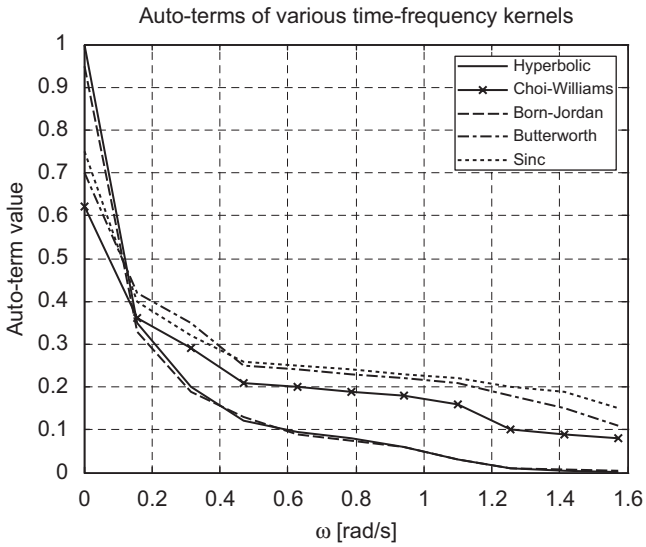

Fig. 8. Auto-terms of hyperbolic, Choi–Williams, Born-Jordan, Butterworth and Sinc time–frequency kernels as functions of ω.

For completeness, noise variance comparisons for the real-noise case of the Born-Jordan, Sinc, hyperbolic, Choi–Williams and Butterworth time–frequency kernels are plotted against the frequency ω (rad/s) in Fig. 8 from which it is clear that the hyperbolic kernel is comparable with the optimal Born-Jordan kernel and is better than the Choi–Williams, Butterworth and Sinc kernels.

6. Conclusions and further work

The lower-bound on SNR of the nth-order hyperbolic kernel has been shown to be in the approximate ranges of -71 to -66 dB for $0 \leqslant a \leqslant 100$, and of -61 to -58 dB for $0 \leqslant \beta \leqslant 70$, with $1 \leqslant n \leqslant 10$. For $n > 10$, the lower-bound on SNR rapidly decreases which suggests that very high-order hyperbolic kernels are not useful. It has been found that the transfer function describing the relationship between the lower-bound on SNR and

the auto-term slope a can be accurately modelled as a seventh-order polynomial by using a 20th-order polynomial fitting method in MATLAB. The transfer function of the lower-bound on SNR and β is a linear function in log–log scales. The function may also be approximately considered as a maximally flat low-pass filter response so that further simplification can be carried out to approximate the hyperbolic kernel family with the Butterworth filter family. The main reason why Butterworth filter family is appropriate in this case is because of the flat pass-band of the transfer function for $0 \leqslant a \leqslant 10$, and its slow roll-off.

It has been found that by examining the lower-bound on SNR as a function of β and n, with a fixed a, the kernel is more noise robust than in the case of fixing β and examining the system as a function of a and n, even though the latter is more performance effective with a higher lower-bound on SNR than the former. The main advantage of the former method is that it makes the kernel family more noise robust as the order n increases. In general, as a further increases, the kernel's SNR decreases which is consistent with findings reported in Ref. [5]. At $n = 7$, the squared weighting function attains its peak, yielding the largest kernel noise variance, and hence the lowest lower-bound on SNR. For $a \geqslant 10$, the lower-bound on SNR sharply decreases.

Further work is currently in progress, focusing on the following four major research directions:

- Modelling of the transfer function relating the lower-bound on SNR to auto-term slope a and to β, in which more thorough investigations using Pade's method and other possible methods are carried out to obtain its pole(s) and zero(s).
- Amplitude modulation of the hyperbolic pulse in noisy conditions because the Fourier transform of a Gaussian-like sech pulse is real.
- Approximation of the hyperbolic kernel family by Butterworth filter family due to the near-flat pass band of the former. Comparisons of the two families are made.
- Detailed investigations on individual members of the hyperbolic kernel family based on a performance benchmark of estimating their noise-robustness ranges. Performance comparisons can then be made.

It should be stressed that some of the above-mentioned research directions can be applied to other different kernels, thus yielding a systematic and convenient comparison of various kernels along with their performances.

Acknowledgements

The author is grateful to the anonymous reviewers for constructive comments which improved the paper. The author would like to thank Dr. K.P. Dabke for carefully proof-reading the manuscript and for helpful discussions.

References

[1] K.N. Le, K.P. Dabke, G.K. Egan, On mathematical derivation of auto-term functions and signal-to-noise ratios of Choi–Williams, first- and nth-order hyperbolic kernels, *Digital Signal Processing: A Review Journal* 16 (1) (2006) 84–104.
[2] H.I. Choi, W.J. Williams, Improved time–frequency representation of multi-component signals using exponential kernels, *IEEE Transactions on Signal Processing* 37 (6) (1989) 862–871.
[3] M.G. Amin, Minimum variance time–frequency kernels for signals in additive noise, *IEEE Transactions on Signal Processing* 44 (9) (1996) 2352–2356.
[4] L. Stankovic, V. Ivanovic, Further results on the minimum variance time–frequency distribution kernels, *IEEE Transactions on Signal Processing* 45 (6) (1997) 1650–1655.
[5] K.N. Le, K.P. Dabke, G.K. Egan, Hyperbolic kernel for time–frequency power spectrum, *Optical Engineering* 42 (8) (2003) 2400–2415.
[6] A.H. Costa, G.F. Boudreaux-Bartels, Design of time–frequency representation using a multiform, tiltable exponential kernel, *IEEE Transactions on Signal Processing* 43 (10) (1995) 2283–2301.
[7] K.N. Le, K.P. Dabke, G.K. Egan, Hyperbolic wavelet power spectra of non-stationary signals, *Optical Engineering* 42 (10) (2003) 3017–3037.
[8] L. Cohen, Time–frequency distribution—a review, *IEEE Proceedings* 77 (7) (1989) 941–981.
[9] L. Cohen, *Time–frequency Analysis*, Prentice-Hall, Englewoods Cliffs, New Jersey, 1995, pp. 136–289.
[10] K.N. Le, K.P. Dabke, G.K. Egan, Hyperbolic wavelet family, *Review of Scientific Instruments* 75 (11) (2004) 4678–4693.
[11] D. Zwillinger, *Standard Mathematical Tables and Formulae*, Chapman & Hall, CRC, New York, 2003, pp. 541–542.